Laser and Particle Beams (2006), *24*, 5–8. Printed in the USA.

DOI: 10.1017/S0263034606060022

Generation and transport of fast electrons inside cone targets irradiated by intense laser pulses

TATSUFUMI NAKAMURA,[1] HITOSHI SAKAGAMI,[2] TOMOYUKI JOHZAKI,[1] HIDEO NAGATOMO,[1] AND KUNIOKI MIMA[1]
[1]Institute of Laser Engineering, Osaka University, Osaka, Japan
[2]National Institute for Fusion Science, Osaka, Japan

(Received 15 June 2005; Accepted 19 September 2005)

Abstract

Fast electrons are effectively generated from solid targets of cone-geometry by irradiating intense laser pulses, which is applied to fast ignition scheme. For realizing optimal core heating by those electrons, understanding the characteristics of electrons emitted from cone targets is crucial. In this paper, in order to understand the generation and transport processes of hot electrons inside the cone target, two-dimensional (2D) particle-in-cell (PIC) simulations were carried out. It is shown that hot electrons form current layers which are guided by self-generated surface magnetic field, which results in effective energy transfer from laser pulse to hot electrons. When the hot electrons propagate through the steep density gradient at the cone tip, electrostatic field is induced via Weibel instability. As a result, hot electrons are confined inside and emitted gradually from the target, as an electron beam of long duration. Energy spectrum and temporal profile of hot electrons are also evaluated at the rear side of the target, where the profile of rear side plasma is taken from the fluid code and the result is sent to Fokker-Planck code.

Keywords: Cone-geometry; Electrostatic field; Fast electrons; Fast ignition; Hot electrons; Solid targets

1. INTRODUCTION

In a fast ignition scenario for inertial confinement fusion, ultra-intense short laser pulse is launched for igniting the core plasma which is produced by implosion laser pulses. The core plasma is surrounded by dense plasma; ignition laser energy is transported by converting them to kinetic energy of high energy charged particles, mainly electrons. The phenomena and problems arising from the fast ignition scheme are a subject of current scientific discussion (Mulser & Schneider, 2004; Mulser & Bauer, 2004; Deutsch, 2004; Pegoraro *et al*., 2004). In recent experiments of fast ignition, three orders increase of neutron yield and core temperature of 800 eV were observed by using a cone-guided target, where a gold cone is irradiated by a PW laser pulse to generate high energy electrons effectively (Kodama *et al*., 2001; Baiwen *et al*., 2004; Malka & Fritzler, 2004). For the further improvements details of physics involved in fast ignition, fast ignition need to be understood. However, the phenomena in fast ignition are complicated and quite diverse ranging from microscopic to macroscopic. Fast ignition integrated interconnecting code project (FI^3 project) is on the way at our institute, where three different simulation codes are being developed to be coupled together in order to simulate the whole process of fast ignition (Sakagami *et al*., 2001; Sakagami & Mima, 2004).

In the FI^3 code, Arbitrary Lagrangian Eulerian (ALE) hydro code (PINOCO) simulates over-all implosion phenomena. Two-dimensional (2D) relativistic Fokker Planck code coupled with Eulerian hydrodynamics (FIBMET) deals with high energy electron transport and core heating process. Hot electron generation process is studied by using Particle-in-Cell (PIC) code (FISCOF1 and FISCOF2). Three codes run independently and exchange data via computer network.

In this paper, we report the results of 2D-PIC simulation part studying the interaction of PW laser pulse and cone target. The purposes of the work are to (1) understand generation and transport processes of hot electrons inside the cone target and (2) obtain electron spectrum propagating out from the rear side of the cone tip, which is used in Fokker-Planck code as the source term of the heating beam.

Address correspondence and reprint requests to: Tatsufumi Nakamura, Institute of Laser Engineering, Osaka University, 2-6 Yamadaoka, Suita-city, Osaka 565-0875, Japan. E-mail: nakamura@ile.osaka.u.ac.jp

Hot electrons are generated at the inner surface of the cone by interacting with intense laser fields and guided by the self-generated surface magnetic field toward the cone tip, which is described in Section 2. In Section 3, hot electron propagation through the cone tip where steep density gradient is localized is analyzed and electron spectrum is presented. Summary and conclusions are given in Section 4.

2. CURRENT LAYER FORMATION AND SURFACE GUIDING BY SELF-GENERATED MAGNETIC FIELD

By irradiating the intense laser pulse onto the cone target, fast electrons are generated at the cone inner-wall by interacting with the laser fields. Since laser fields penetrate only up to critical density or more precisely the effective critical density modified by relativistic mass correction that is, $n_{ceff.} = \gamma n_{cr} (n_{cr} = \omega_0^2 m\varepsilon_0/e^2$, where ω_0 is laser frequency, ε_0 is permittivity, and e is electric charge), hot electron generation by laser–cone interaction is localized at the solid target surface. Thus we use cone target of 20 times the critical density ($n_e = 20\ n_{cr}$) and of being isolated that is, without corona plasma at the rear side throughout this section for studying the generation and transport processes of hot electrons inside the cone.

Simulation box size is about 10 μm in x-directions (laser incident direction) and 12 μm in y-direction. The laser field is assumed to be polarized in the y-direction. The peak laser intensity is 4×10^{19} W/cm^2 which corresponds to $a = 6$ where $a = \mathrm{eA/mc}$ is the normalized vector potential, and the laser wavelength is 1 μm. The focal diameter is 4 μm with Gaussian in radial direction. The laser pulse has semi-infinite duration which rises up in five times the laser period and maintains its intensity. The cone target consists of electrons and immobile ions. The initial electron temperature is 10 keV.

The current density of x-component is plotted in Figure 1. Three lines in the figure express the density contour of n_{cr}, 6 n_{cr} which is effective critical density, and 20 n_{cr}. The forward current is drawn in black that flows in effective underdense region where laser field can interact with electrons, and return current which is drawn in white flows in overdense region. The generated hot electrons are well organized and confined in a narrow layer along the surface. This structure is quite beneficial for fast ignition since electrons are effectively accelerated towards the cone tip. Also, the structure is unique, since in cases of normal incident or incident with smaller angle, electrons are accelerated in the direction of laser wave vector and form current filaments via Weibel instability, where electron motion is disturbed as well as magnetic field structure (Sheng *et al.*, 2000; Sentoku *et al.*, 2002; Wilks *et al.*, 1992; Haines, 1986). In cone target case, electron motion is organized and guided by static magnetic field which is plotted in Figure 2. The maximum magnitude of surface magnetic field is about 200 MG which is about 30% of the laser magnetic field. This huge magnetic field prevents hot electrons which are pushed pondromotively by laser fields from penetrating into the target. The electrons are bent toward vacuum side by the magnetic field and dragged back to the target by electrostatic field, and interact with the magnetic field again. This electron motion accounts for a surface current which enhances the surface magnetic field. In this configuration which is considered as a steady-state of non-equilibrium open system, the absorbed laser energy is transported away from the

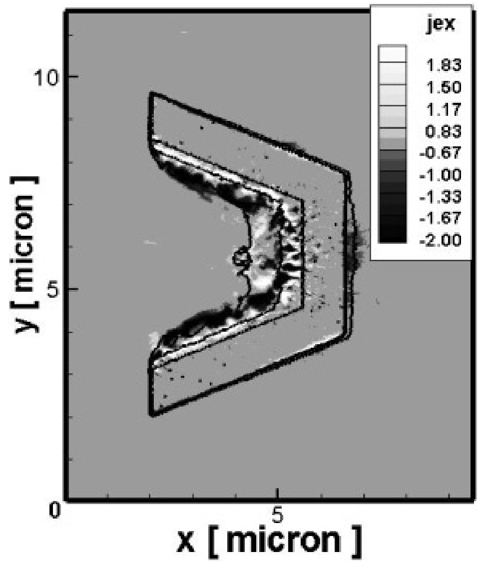

Fig. 1. Distribution of current density of x-component. Forward current layer is formed in underdense region and return current flows above the effective critical density region. The quantity is normalized by $e\, n_{cr}\, c$ which corresponds to 5×10^{16} A/m^2 in this simulation.

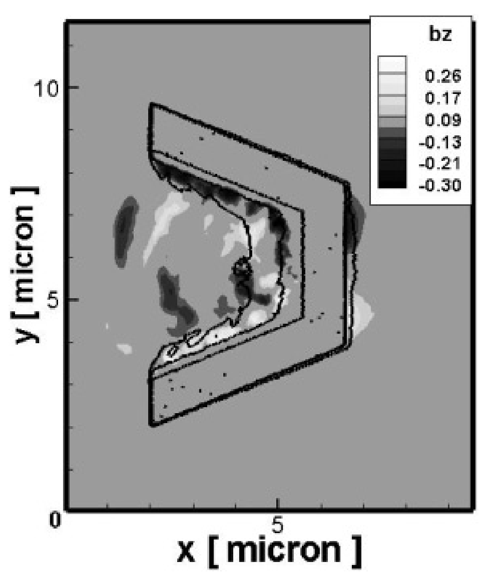

Fig. 2. Profile of magnetic field which is averaged over the laser period and normalized by laser magnetic field B_L. The Maximum magnitude of surface magnetic field is about 200 MG.

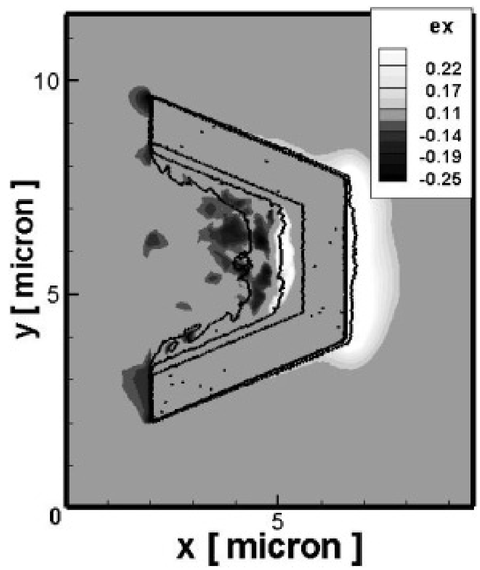

Fig. 3. Electro-static field induce at the tip of the cone tip. The field is normalized with laser electric field.

interaction region constantly by hot electrons flow, and this energy flow sustains the surface magnetic field (Nakamura *et al*., 2004). Thus this structure is considered to be robust and easily seen at solid surface obliquely irradiated by intense laser fields. The magnitude of surface magnetic field strongly depends on the laser incident angle.

As a result, current layer is formed and flows along the target surface toward the cone tip. The average surface current density becomes up to 10^{17} A/m^2 and the magnitude of the surface magnetic field becomes up to 200 MG which is about 30% of the laser magnetic field.

3. ELECTRON BEAM TRANSPORT THROUGH CONE TARGET

The hot electrons transported in the underdense region along the target surface flow to the tip of the cone. At the cone tip there exists steep density gradient and electrons cannot penetrate smoothly into the overdense region. As is seen in Figure 1, current layers break into small filaments as they penetrate into the target via Weibel or filamentation instability (Bret *et al*., 2005; Deutsch *et al*., 2005). Electrons lose their energy and background electrons are heated due to the anomalous resistively (Deutsch, 2004; Sentoku *et al*., 2003). As a result, electrostatic field is induced at the boundary as is shown in Figure 3. Similar phenomena are observed in one-dimensional (1D) PIC simulation of laser-solid interaction (Sakagami *et al*., 2006; Passoni & Lontano, 2004), where two-stream instability grows at the steep density gradient which results in inducing a strong electro-static field at the boundary. Hot electrons are prevented from smoothly propagating into and out of the target.

In order to evaluate the electron spectrum propagating out from the target, we performed simulation on cone target whose density is 100 times the critical density. Also, as the density gradient plays important role in beam propagation, the effect of core surrounding plasma is taken into account. The hydro simulation (PINOCO) revealed that between the cone target and core plasma there exist large scale plasma of slight overdense. The density changes from 2 to 10 times the critical density depending on time. At the time which is considered as optimum timing for launching the ignition laser pulse, the rear side plasma density is evaluated as 2 n_c. Thus we use target of cone geometry which is same size as before, and to which uniform plasma whose density is 2 n_c is attached at the rear side. The plasma consists of electrons and immobile ions whose initial temperatures are 10 KeV and 0, respectively. Laser pulse has Gaussian profile in radial direction with a focal diameter of 4 μm, and also Gaussian temporal profile with duration of 150 fs with FWHM. The peak intensity is 4×10^{19} W/cm^2 and wavelength is 1 μm.

The characteristics of electron beam coming out from the cone target are shown in Figure 4. In the left figure, electron spectrums of forward-going electrons observed inside and outside of the cone are plotted when the center of the laser pulse having peak intensity has reached at the target. The

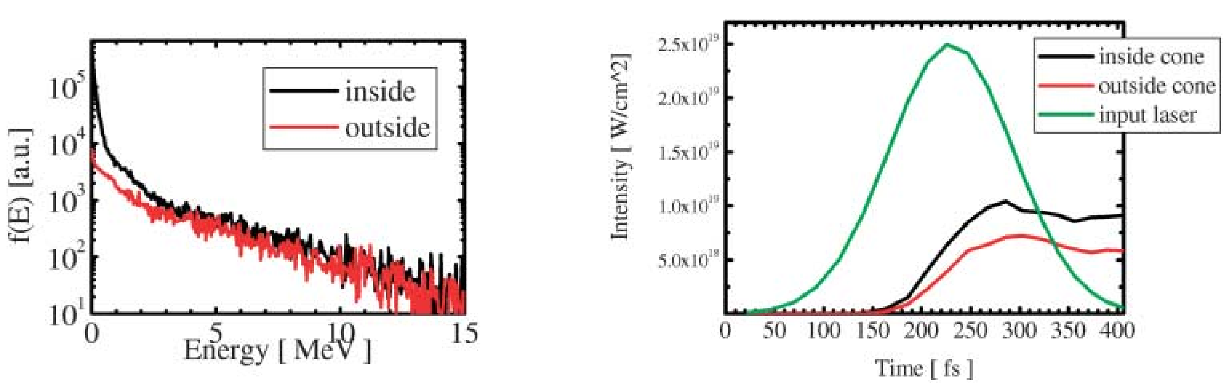

Fig. 4. Electron spectrum at rear side and inner side of the cone (left), and temporal profile of electron beam intensity (right).

https://doi.org/10.1017/S0263034606060022 Published online by Cambridge University Press

observing points are set 1 μm inner side and outer side from the rear edge of the cone. The both spectrums are similar for high energy electrons, whose effective temperatures are scaled by ponderomotive energy (Wilks, 1993; Chen & Wilks, 2005). The abundant electrons with lower energy inside the target mean that electrons are confined inside due to electrostatic field which is induced at the rear boundary. The magnitude of electrostatic field at the rear side of the cone becomes comparable to the laser electric field. These confined electrons are emitted from the target even after laser pulse is turned off. The temporal profile of electron beam observed at 1 μm rear side of the boundary is shown in the right figure. There is a net energy flow in forward direction since the intensity of the forward electron beam is always larger than the backward beam and the beam duration is longer than the input laser pulse. The hot electrons are stopped by the electrostatic field at the boundary, but converted to rather long-lasting beam. The obtained electron spectrum is used to evaluate energy transport through corona plasma and energy deposition at core plasma, where Fokker-Planck simulation is used since collisional effects play important role. The detailed analysis of core heating by Fokker-Planck code is going on, and will be given in the near future. Ions are emitted from the target in a long run, which will also be included in the following work.

4. CONCLUSION

Hot electrons are generated at the inner surface of the cone and guided by static electromagnetic fields toward the tip of the cone, where magnitude of surface magnetic field becomes up to about 30 percent of laser magnetic field. The electrostatic field is induced at the sharp density gradient via Weibel or two-stream instability, which confines electrons with moderate energy. Thus the duration of electron beam becomes longer than the input laser pulse and is expected to heat the core effectively.

REFERENCES

Baiwen, L., Ishiguro, S., Skoric, M.M., Takamaru, H. & Sato, T. (2004). Acceleration of high-quality, well-collimated return beam of relativistic electrons by intense laser pulse in a low-density plasma. *Laser Part. Beams* **22**, 307–314.

Bret, A., Firpo, M.C. & Deutsch, C. (2005). Characterization of the initial filamentation of a relativistic electron beam passing through a plasma. *Phys. Rev. Lett.* **94**, 115002.

Chen, H. & Wilks, S.C. (2005). Evidence of enhanced effective hot electron temperatures in ultraintense laser-solid interactions due to reflexing. *Laser Part. Beams* **22**, 411–416.

Deutsch, C. (2004). Penetration of intense charged particle beams in the outer layers of precompressed thermonuclear fuels. *Laser Part. Beams* **22**, 115–120.

Deutsch, C., Bret, A. & Fromy, P. (2005). Mitigation of electromagnetic instabilities in fast ignition scenarios. *Laser Part. Beams* **23**, 5–8.

Haines, M.G. (1986). Magnetic-field generation in laser fusion and hot-electron transport. *Can. J. Phys.* **64**, 912–919.

Kodama, R., Norreys, P.A., Mima, K., Dangor, A.E., Evans, R.G., Fujita, H., Kitagawa, Y., Krushelnick, K., Miyakoshi, T., Miyanaga, N., Norimatsu, T., Rose, S.J., Shozaki, T., Shigemori, K., Sunahara, A., Tampo, M., Tanaka, K.A., Toyama, Y., Yamanaka, Y. & Zepf, M. (2001). Fast heating of ultrahigh-density plasma as a step towards laser fusion ignition. *Nature* **412**, 798–802.

Malka, V. & Fritzler, S. (2004). Electron and proton beams produced by ultra short laser pulses in the relativistic regime. *Laser Part. Beams* **22**, 399–405.

Mulser, P. & Bauer, D. (2004). Fast ignition of fusion pellets with superintense lasers: Concepts, problems, and prospectives. *Laser Part. Beams* **22**, 5–12.

Mulser, P. & Schneider, R. (2004). On the inefficiency of hole boring in fast ignition. *Laser Part. Beams* **22**, 157–162.

Nakamura, T., Kato, S., Nagatomo, H. & Mima, K. (2004). Surface-magnetic-field and fast-electron-layer formation by ultra-intense laser irradiation. *Phys. Rev. Lett.* **93**, 265002.

Passoni, M. & Lontano, M. (2004). One-dimensional model of the electrostatic ion acceleration in the ultraintense laser-solid interaction. *Laser Part. Beams* **22**, 163–169.

Pegoraro, F., Atzeni, S., Borghesi, M., Bulanov, S., Esirkepov, T., Honrubia, J., Kato, Y., Khoroshkov, V., Nishihara, K., Tajima, T., Temporal, M. & Willi, O. (2004). Production of ion beams in high-power laser-plasma interactions and their applications. *Laser Part. Beams* **22**, 19–24.

Sakagami, H. & Mima, K. (2004). Interconnection between hydro and PIC codes for fast ignition simulations. *Laser Part. Beams* **22**, 41–44.

Sakagami, H., et al. (2001). *Fast Ignition Simulations with Collective PIC Code*. pp. 380–383. Paris: Elsevier.

Sakagami, H., Johzaki, T., Nagotomo, H. & Mima, K. (2006). Fast ignition integrated interconnecting code project for cone-guided targets. *Laser Part. Beams* **24**, 191–198.

Sentoku, Y., Mima, K., Kaw, P. & Nishikawa, K. (2003). Anomalous resistively resulting from Mev-electron transport in overdense plasma. *Phys. Rev. Lett.* **90**, 155001.

Sentoku, Y., Mima, K., Sheng, Z.M., Kaw, P., Nishihara, K. & Nishikawa, K. (2002). Three-dimensional particle-in-cell simulations of energetic electron generation and transport with relativistic laser pulses in overdense plasmas. *Phys. Rev. E* **65**, 046408.

Sheng, Z.M., Sentoku, Y., Mima, K., Zhang, J., Yu, W. & Meyer-ter-Vehn, J. (2000). Angular distributions of fast electrons, ions, and bremsstrahlung X/gamma-rays in intense laser interaction with solid targets. *Phys. Rev. Lett.* **85**, 5340–5343.

Wilks, S.C., Kruer, W.L., Tabak, M. & Langdon, A.B. (1992). Absorption of ultra-intense laser pulses. *Phys. Rev. Lett.* **69**, 1383.

Wilks, S.C. (1993). Simulations of ultraintense laser-plasma interactions. *Phys. Fluids B.* **5**, 2603.